In vitro degradation and in vivo resorption of dicalcium phosphate cement based grafts

Sheikh, Zeeshan; Zhang, Yu Ling; Grover, Liam; Merle, Géraldine E.; Tamimi, Faleh; Barralet, Jake

DOI:
10.1016/j.actbio.2015.08.031

Document Version
Peer reviewed version

Citation for published version (Harvard):
Sheikh, Z, Zhang, YL, Grover, L, Merle, GE, Tamimi, F & Barralet, J 2015, 'In vitro degradation and in vivo resorption of dicalcium phosphate cement based grafts', *Acta Biomaterialia*, vol. 26, pp. 338-346. https://doi.org/10.1016/j.actbio.2015.08.031

Accepted Manuscript

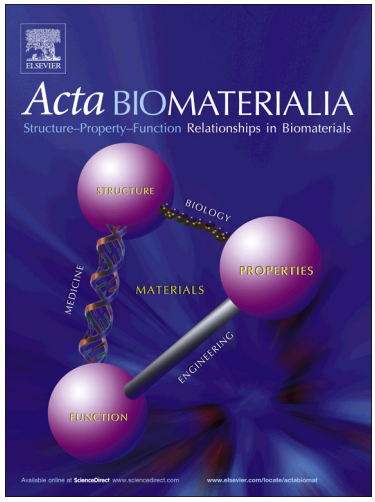

In vitro degradation and *in vivo* resorption of dicalcium phosphate cement based grafts

Zeeshan Sheikh, Yu Ling Zhang, Liam Grover, Géraldine Merle, Faleh Tamimi, Jake Barralet

PII: S1742-7061(15)30075-1
DOI: http://dx.doi.org/10.1016/j.actbio.2015.08.031
Reference: ACTBIO 3845

To appear in: *Acta Biomaterialia*

Received Date: 19 June 2014
Revised Date: 16 July 2015
Accepted Date: 19 August 2015

Please cite this article as: Sheikh, Z., Zhang, Y.L., Grover, L., Merle, G., Tamimi, F., Barralet, J., *In vitro* degradation and *in vivo* resorption of dicalcium phosphate cement based grafts, *Acta Biomaterialia* (2015), doi: http://dx.doi.org/10.1016/j.actbio.2015.08.031

In vitro degradation and *in vivo* resorption of dicalcium phosphate cement based grafts

Zeeshan Sheikh. [a]Faculty of Dentistry, McGill University. 3640, Strathcona Anatomy and Dentistry Building, Rue University. Montreal. Quebec, H3A 0C7. Canada. (zeeshan.sheikh@mail.mcgill.ca)

Yu Ling Zhang. [a]Faculty of Dentistry, McGill University. 3640, Strathcona Anatomy and Dentistry Building, Rue University. Montreal. Quebec, H3A 0C7. Canada. (yu.l.zhang@mcgill.ca)

Liam Grover. [b]School of Chemical Engineering, University of Birmingham, Edgbaston, Birmingham, B15 2TT. UK.
(l.m.grover@bham.ac.uk)

Géraldine Merle [a]Faculty of Dentistry, McGill University. 3640, Strathcona Anatomy and Dentistry Building, Rue University. Montreal. Quebec, H3A 0C7. Canada. (geraldine.merle@mcgill.ca)

Faleh Tamimi. [a]Faculty of Dentistry, McGill University. 3640, Strathcona Anatomy and Dentistry Building, Rue University. Montreal. Quebec, H3A 0C7. Canada. (faleh.tamimimarino@mcgill.ca)

Jake Barralet. [a]Faculty of Dentistry, McGill University. 3640, Strathcona Anatomy and Dentistry Building, Rue University. Montreal. Quebec, H3A 0C7. Canada.
[c]Division of Orthopaedics, Department of Surgery, Faculty of Medicine,
McGill University, 1650 Cedar Ave, Montreal General Hospital. Montreal, Quebec, H3G 1A4. Canada.
(jake.barralet@mcgill.ca)

Corresponding author: Jake Barralet.
[a]Faculty of Dentistry, McGill University. 3640, Strathcona Anatomy and Dentistry Building, Rue University. Montreal. Quebec, H3A 0C7. Canada.
[c]Division of Orthopaedics, Department of Surgery, Faculty of Medicine,
McGill University, 1650 Cedar Ave, Montreal General Hospital. Montreal, Quebec, H3G 1A4. Canada.
e-mail address: jake.barralet@mcgill.ca
Tel.: +1 5143987203

Abstract

Dicalcium phosphates (DCP) are calcium phosphates and there are two types of DCP: dihydrated (brushite) and unhydrated (monetite). After implantation, brushite converts to hydroxyapatite (HA) which resorbs very slowly. This conversion is not observed after implantation of monetite cements and results in greater resorption. The mechanisms of resorption and degradation however of these ceramics remain largely unknown. This study was designed to investigate the effect of: porosity, surface area and hydration on *in vitro* degradation and *in vivo* resorption of DCP. Brushite and two types of monetite cement based grafts (produced by wet and dry thermal conversion) were aged in phosphate buffered saline (PBS), bovine serum solutions *in vitro* and implanted subcutaneously in rats. Here we show that for high porosity grafts (50-65%), solubility and surface area does not play a significant role towards *in vitro* mass loss with disintegration and fragmentation being the main factors dictating mass loss. For grafts having lower porosity (35-45%), solubility plays a more crucial role in mass loss during *in vitro* ageing and *in vivo* resorption. Also, serum inhibited dissolution and the formation of HA in brushite cements. However, when aged in PBS, brushite undergoes phase conversion to a mixture of octacalcium phosphate (OCP) and HA. This phase conversion was not observed for monetite upon ageing (in both serum and PBS) or in subcutaneous implantation. This study provides greater understanding of the degradation and resorption process of DCP based grafts, allowing us to prepare bone replacement materials with more predictable resorption profiles.

Keywords: Cements; Brushite; Monetite; Dicalcium phosphate; In vivo resorption; In vitro degradation.

1. Introduction

Dicalcium phosphates (DCP) are calcium phosphates of great interest for orthopaedic and dental applications. Brushite cements set via a dissolution/precipitation process at low pH (<6) [1, 2]. One of methods by which brushite cements can be prepared is by mixing an acidic calcium phosphate such as monocalcium phosphate monohydrate (MCPM) and a basic calcium phosphate like beta tricalcium phosphate (β-TCP) with water. This method results in a moldable paste that sets into a solid cementitious material composed mainly of dicalcium phosphate dihydrate (DCPD) [3-5]. Brushite cements can also be utilized as precursors to the anhydrous form of dicalcium phosphate (DCPA), also known as monetite. Brushite crystals when heated above 60°C start to dehydrate into monetite [6], and if moisture is maintained during the heating process (as in autoclaving) then bulk shrinkage is prevented and an increase in the internal pore size is observed [7]. This conversion into monetite can also be carried out by dry heating the preset brushite cements [8]. These wet and dry heat conversions of brushite to monetite results in two materials that are chemically very similar yet differ with respect to physical properties (total porosity, pore size distribution, density and surface area) [8, 9].

The success of bone replacement procedures is limited by the low or negligible resorption rates associated with the use of calcium phosphate cements [2]. A significant reduction in the rate of resorption is frequently reported due to the phase conversion of brushite to hydroxyapatite (HA) [10, 11]. It has been observed that monetite does not re-

precipitate into HA *in vivo*, and recent research demonstrates its good osteoconductive and osteoinductive properties [8, 9, 12-15].

Studies investigating behaviour of brushite cements after implantation or immersion in aqueous media have reported resorption, disintegration or long-term stability [16-18]. Brushite cements have been shown to exhibit a decrease in mass, an increase in porosity, and a deterioration in mechanical properties upon *in vitro* incubation [19]. It has been reported that cement porosity, as well as the properties of surrounding medium and the rate of fluid exchange affects initial brushite resorption [20]. Disintegration and fragmentation of cement matrix rather than simple dissolution can also contribute to mass loss during brushite incubation *in vitro* [20].

Brushite cements have been shown to experience an initially linear degradation rate of 0.25 mm per week once implanted *in vivo* [16]. However, degradation rate is dependent on a variety of factors such as: cement physico-chemical properties, species of animal in which implanted site of implantation and blood flow. After implantation, during initial few weeks brushite cements appear to resorb by disintegration, simple dissolution and cellular activity (macrophages and osteoclasts) [17, 21, 22]. It has also been observed that serum can adsorb onto cement surface altering the interfacial properties promoting brushite resorption *in vivo* and *in vitro* [20]. The resorption mechanism of monetite is similar to that observed for brushite cement grafts, in that it is mainly mediated by cellular activity and simple dissolution [23]. Recent studies have shown that monetite grafts produced by autoclaving of preset brushite cements appear to resorb more in comparison to the original brushite grafts [9, 24].

In this study, brushite cement grafts were prepared and monetite grafts obtained from them via wet heat and dry heat conversion. The *in vitro* and *in vivo* behaviour of these grafts was investigated by ageing in phosphate buffered saline (PBS) and bovine serum solutions and also subcutaneous implantations in rats. We attempted to discern the effect of DCP hydration, porosity and surface area on *in vitro* and *in vivo* degradation and resorption.

2. Method and materials

2.1 Synthesis

Brushite cement grafts were prepared with a mixture of β-TCP (Merck) and commercially available monocalcium calcium phosphate monohydrate (MCPM) (ABCR, GmbH & Co.KG) using a ratio of 1.2 to 1 respectively. In order to investigate the effect of powder to liquid (P/L) ratio on physical properties and degradation, brushite and monetite cements were produced at P/L mixing ratio of 3 and 1 g/ml. The powders were hand ground with a pestle and mortar and cement pastes prepared by mixing the powder with appropriate amount of distilled water on a glass slab for 20 s. Once all of the powder was combined with the liquid, the cement paste was kneaded for a further 30 s. The manipulated cement slurry was cast into a polytetrafluoroethylene (PTFE) split mould forming hardened cement cylinders Ø (~12 mm (height) x 6 mm (diameter)). The cylinders were allowed to set for 24 h at 37°C ± 1˚C in a vacuum desiccator to form hard brushite. At the end of the incubation period, the samples were removed from the mould and weighed until constant mass was reached. Five different batches of thirty cylinders each were produced to obtain a total of one hundred and fifty cylinders with 3 and 1 P/L

ratios. Even though samples were prepared using same protocol, the sample assignment was randomized to minimize variations.

Monetite cement grafts (n=70 in total) were synthesized by conversion of the preset brushite cement cylinders utilizing two different methods: thermal and hydrothermal conversion. For thermal conversion, the brushite cylinders (n=35) were dry heated at 250°C for 30 minutes under vacuum (80 mTorr). Hydrothermal transformation was performed with the brushite cylinders (n=35) being autoclaved at sterilizing conditions (120°C, 100% humidity and 15 psi, for 30 min).

2.2 Characterisation

The phase purity of the prepared brushite and the monetite grafts was confirmed using X-ray diffraction (XRD). XRD data was collected (Bruker Discover D8 diffractometer) from the surface of the graft materials with Ni filtered CuKα radiation (λ = 1.54A) with a two dimensional VANTEC area detector at 40 kV and 40 mA. A step size of 0.02° was used to measure from 10 to 50° 2θ over 3 frames with a count time of 300 s per frame. The phase composition was compared and confirmed with the International Centre for Diffraction Data reference patterns for brushite (PDF Ref. 09-0077) and monetite (PDF Ref. 09-0080), JCPDS 2010 database.

The compressive strength of all prepared grafts was measured before and after *in vitro* ageing and subcutaneous implantation. Before testing, geometrical measurements of the graft cylinders were made in triplicate and the samples weighed. Samples were mounted on the testing machine (5544, Instron) so that the long axes of the cement cylinders were

perpendicular to the lower anvil. A compressive force was then applied to the upper surface of the cylinders at a constant crosshead displacement rate of 1 mm/min until failure occurred. The applied load was measured using a 100 N load cell (5544, Instron). Mean compressive strength was determined from the average of 10 measurements.

After testing in compression, cement fragments were retrieved, weighed and dried in a vacuum desiccator at a temperature of 37°C. The fragments were then ground to powder using a pestle and mortar. The true density of the powdered grafts was determined using a helium pycnometer (Accupyc 1330, Micromeritics). The volume of each sample was measured 10 times following 10 purges of the measurement chamber with helium. The relative porosity (bulk porosity) of the cements was calculated from apparent and true density measurements. The specific surface area (SSA) of the cement grafts in their solid cylindrical form was determined by using the Brunauer–Emmett–Teller (BET) method with helium adsorption–desorption (Tristar3000, Micromeritics).

Bioceramic microstructure was observed using scanning electron microscopy (SEM) (Hitachi S-4700 FE-SEM; Tokyo, Japan), at an accelerating voltage of 2 kV. Elemental composition of the bioceramics was assessed with energy dispersive X-ray (EDX) analysis using Oxford detector and INCA software (Oxford Instruments, Abingdon, UK). The pore size distribution of the prepared brushite and monetite cement grafts prior to *in vitro* and *in vivo* experiments was measured by using mercury intrusion porosimetry (9420, Micromeritics, Bedfordshire, UK).

2.3 In vitro ageing

After initial characterisation was complete, the graft cylinders were stored at 37 ± 1°C and ~100% relative humidity for 24 h. Brushite and the autoclaved and dry heat monetite grafts (*n=3*) were immersed in PBS solutions (MP Biomedicals, LLC. Solon, OH. Cat no: 2810305), and also in bovine serum (Gibco, product code:16170, New Zealand) containing sodium azide (Sigma-Aldrich) at a concentration of 0.1%. The graft cylinders were aged at a liquid to cement volume ratio (LCVR) of 60 as used by Grover et al. [20] for 7, 30 and 60 days at 37 ± 1°C. Dynamic ageing protocols were achieved by refreshing the liquid every 24 h throughout the experiment to remove any dissolution products. To quantify the amount of mass loss over time, the graft cylinders were removed daily from the ageing medium and weighed. After periods of 7, 30 and 60 days of ageing, the grafts were removed from the solutions and tested in compression and characterised for changes in phase composition, SSA, density and porosity. A repeat experiment was performed to examine fragment composition from monetite grafts in serum. As soon as sufficient material for characterization had formed (3 weeks) the fragments were washed and dried before SEM and XRD analyses.

2.4 Animal study

The surgical protocol for animal testing for research was approved by the McGill University Ethical Committee (Animal use protocol # 6020). For evaluation of bio-resorption and changes in the physicochemical properties *in vivo*, the prepared calcium phosphate grafts were implanted subcutaneously in rats (*n=6*). 36 male Wistar rats (35-40 days old, 126-150 g weight) were purchased from Charles River Laboratories, Montreal, Quebec, Canada. Briefly, two subcutaneous pockets on either side in the flanks of the

animals were accessed via a mid-scapular surgical incision. The implants were placed (unfixed) into the pocket. It was ensured using blunt dissection that the subcutaneous pocket is made and that the graft does not rest directly beneath the incision, as this could have potentially interfered with wound healing. After placement of grafts in their respective pockets, the incision was closed using resorbable monocryl sutures. After 4 and 12 weeks of implantation, animals were sacrificed and implants retrieved. Digital radiographs were obtained using Kubtec® XPERT80 X-ray system (KUB Technologies Inc. Milford, CT) employing a voltage of 90 kV and a tube current of 1.0 µa. The retrieved grafts were tested in compression, characterised for changes in phase structure, SSA, density, porosity and mass loss.

2.5 Statistical analysis

Statistical analysis was performed using the statistical software IBM®SPSS® (v. 19, IBM SPSS Inc., Chicago, IL). Statistical significance between groups was determined by non-parametric analysis with *Wilcoxon sign rank test* ($p < 0.05$).

3. Results

3.1 Mechanical properties of the prepared grafts

The powder to liquid ratio (P/L ratio) employed to prepare brushite and monetite grafts had a marked influence on compressive strength. The compressive strength approximately doubled when the P/L ratio for brushite grafts was increased from 1 to 3 g/ml (Table 1). An approximate three-fold increase and a four-fold increase was observed when the P/L ratio was increased from 1 to 3 for the dry heat and autoclave converted

monetite grafts respectively (Table 1). The increase in compressive strength of brushite grafts when the P/L ratio was increased from 1 to 3 was associated with a reduction in the relative porosity from ~65% to ~36%. Similar effects of reduction in relative porosity with increase in the P/L ratio were observed for the dry heat monetite and autoclaved monetite grafts.

3.2 Pore size evaluation of the prepared grafts

Mercury porosimetry of the grafts prepared with a P/L mixing ratio of 3 prior to immersion in PBS, serum and subcutaneous implantation showed that the diameter of the majority of pores were between ~500 nm and ~600 nm for brushite, ~800 nm to ~1 µm for autoclaved monetite, and ~700nm to ~1 µm for the dry heat monetite (Fig. 1). The results for the 1:1 P/L ratio grafts revealed bimodal pore diameter distribution with modal values of ~4 µm and ~9 µm for brushite, ~5 µm to ~8 µm for autoclaved monetite, and ~3 µm to ~8 µm for the dry heat monetite (Fig. 1).

3.3 Mass loss quantification after subcutaneous implantation and in vitro ageing

Upon visual inspection and mass loss quantification of the retrieved grafts (prepared with P/L ratio of 3) from rats, brushite explants after 4 weeks of implantation showed slightly less resorption (~6%) (Fig. 2a) in comparison to the dry heat (~9%) (Fig. 2b) and autoclaved (~12%) (Fig. 2c) monetite explants. Similar observations were made for the brushite (~17%) (Fig. 2d), dry heat monetite (~25%) (Fig. 2e), and autoclaved monetite (~30%)(Fig. 2f) grafts retrieved after 12 weeks. The radiographs obtained from the

animals after implantation of the grafts (Fig. 2g), after 4 weeks (Fig. 2h), and after 12 weeks (Fig. 2i) also demonstrated the visual difference in the extent of resorption between brushite and the monetite grafts *in vivo*.

All grafts aged in serum showed a greater loss of mass over 60 days when compared to ageing in PBS ($P < 0.05$) (Table 2 and Fig. 6). Brushite grafts prepared with P/L ratio of 3 after 26 days of ageing in PBS started to lose more mass daily and this trend continued till about day 56 (Fig. 6a). After day 56, the brushite seemed to have stopped losing mass (Fig. 6a). When this was compared with the results from the *in vitro* ageing in serum for the 3:1 P/L ratio grafts, we observed that brushite lost mass continuously till day 60 (Fig. 6b). When the 1:1 P/L ratio grafts were aged in PBS and serum, they lost similar amount of mass (~10%) during the first 10 days (Fig. 6c & d). However after the first 10 days, the grafts aged in serum continued to lose more mass daily over the next 50 days. The 1:1 P/L ratio grafts being more porous than their 3:1 P/L ratio counterparts demonstrated a quicker rate of disintegration (Fig. 6c & d). In comparison, the 3:1 P/L ratio grafts underwent less fragmentation and maintained physical integrity better. The difference in the mechanical properties of these grafts also matches with this observation, since 3:1 P/L ratio grafts had higher compressive strength when compared with the 1:1 P/L ratio grafts (Table 1). The 3:1 P/L ratio grafts aged in PBS showed minimal mass loss for the first 26 days (~2.5%). Autoclaved monetite grafts continued to lose mass at a similar rate for the next 34 days and at the end lost ~4.5% of its starting mass. Autoclaved monetite demonstrated the greatest amount of *in vivo* resorption ($P < 0.05$) followed by dry heat monetite grafts, while the least amount of resorption was shown by brushite grafts for the similar P/L ratios employed (Table 2 and Fig. 7).

3.4 XRD phase analysis

Phase analysis via XRD confirmed that the bioceramic grafts were comprised of brushite after setting, and that the autoclaving and dry heating processes resulted in conversion of brushite to monetite (Fig. 3 and Fig. 4). The brushite grafts aged in PBS showed phase conversion from brushite to a mixture of octacalcium phosphate (OCP) and HA after 60 days (Fig. 3). In order to confirm the presence of OCP XRD patterns were recorded from 3° 2θ and the characteristic intense peak of OCP at 4.75 °2θ was observed (Fig. S7). The brushite grafts aged in serum did not show phase change at any time point (data not shown). Similar results were obtained for the brushite grafts after 4 weeks of implantation with no phase change observed. A mixture of OCP and HA peaks were seen in the XRD patterns of the surface of brushite at 12 weeks *in vivo* but not for the core (Fig. 4). The monetite cement grafts (autoclaved and dry heated), aged *in vitro*, and implanted subcutaneously, did not show any phase change or conversion to apatite when characterised after 4 and 12 weeks (surface and core analysed for 12 week time point) (Fig. 3 and Fig. 4).

3.5 SEM analysis

SEM micrographs were obtained from the surface of all grafts prior to and after implantation and ageing. The prepared brushite grafts showed blade like crystals in the ~5 µm size range (Fig. 5a). When aged in PBS, the brushite grafts showed blade or

needle like crystal growth of OCP (Fig. 5b). When the same brushite grafts were aged in serum, smaller crystals were observed with the size being less than 2-3 µm (Fig. 5c). Subcutaneously implanted brushite grafts showed similar blade like crystal morphology of OCP (Fig. 5d). These microstructural observations were consistent irrespective of P/L ratio used to prepare the bioceramics. The primary crystal morphology of the autoclaved monetite grafts when prepared showed crystals mostly in the ~2-4 µm size range (Fig. 5e). After ageing in serum, the microstructure of autoclaved monetite grafts changed to ~1 µm in size (Fig. 5g). Autoclaved monetite grafts aged in PBS solution and implanted subcutaneously also showed small sized crystals (Fig. 5f & 5h). The dry heat monetite grafts prepared for the ageing experiments and implantations had mostly extremely small crystals with size smaller than 1 µm (Fig. 5i). After ageing in PBS, we observed similar crystal morphology with the original grafts yet the crystal size had become smaller (Fig. 5j). It was interesting to note the appearance of the dry heat graft microstructure after ageing in serum as the original brushite crystal morphology seemed to have been maintained but they had transformed into porous assemblies of nanocrystals (Fig. 5k). After subcutaneous implantation the dry heat monetite grafts showed an appearance which was a mixture of that seen in the PBS aged samples (smaller crystals) and the subcutaneously implanted samples (porous blocks) (Fig. 5k). No blade like crystals of OCP were observed in any of the monetite grafts after being in PBS, serum or *in vivo* for any given time period.

3.6 Elemental analysis

Elemental analysis of the bioceramics revealed that brushite and both the autoclaved and dry heat monetite grafts had a similar calcium-to-phosphate (Ca/P) ratio, slightly higher than 1.0 (Table 3). However when the samples were aged in PBS and implanted subcutaneously it was observed that the Ca/P ratio for brushite grafts increased, matching closely to the Ca/P ratio expected for OCP (1.33). This increase was not observed for the grafts aged in serum. The autoclaved and dry heat monetite grafts did not show significant changes in the Ca/P ratio after being aged in PBS or implanted (Table 3).

4. Discussion

4.1 *In vitro* dissolution & *in vivo* resorption

Passive dissolution, fragmentation, cellular activity and phase conversion are the key mechanisms that determine the rate and amount of mass loss from brushite cements during *in vitro* incubation and *in vivo* implantation [20, 25, 26]. Dissolution occurs when brushite is placed in an environment that is under saturated in calcium and phosphate ions and proceeds according to the following equation:

$$CaHPO_4 \cdot 2H_2O \rightarrow Ca^{2+} + HPO_4^{2-} + 2H_2O \qquad (1)$$

The process of dissolution stops once the solubility limit has been reached [19, 20, 27]. Brushite dissolution supersaturates the environment with respect to HA, ultimately resulting in HA precipitation (possibly non-stoichiometric). Brushite conversion to HA occurs via two steps; dissolution and precipitation [28] and proceeds according to the following equation:

$$10CaHPO_4 \cdot 2H_2O \rightarrow Ca_{10}(PO_4)_6(OH)_2 + 4H_3PO_4 + 18H_2O \qquad (2)$$

Once the cement was immersed in ageing media, the process of brushite dissolution could begin immediately since PBS used in our study contained no calcium ions. This would be expected to increase calcium and phosphate ion concentration, resulting in reduction of cement dissolution rate. By removing the dissolution products on a daily basis a relatively higher rate of dissolution was maintained, analogous to the *in vivo* process of fluid turn over.

Phase conversion to OCP and HA along with limited mass loss observed for brushite grafts aged in PBS match with the results obtained from same grafts after subcutaneous implantation (Fig. 3 & 4). It is already known that the Ca/P ratio of OCP and HA are 1.33 and 1.67 respectively [8, 9]. The Ca/P ratio noted for the PBS aged and subcutaneously implanted brushite grafts was between these two values indicating a mixed phase content of the remaining cement. In a previous study, brushite cement set by mixing β-TCP with orthophosphoric acid showed the presence of HA after 14 days of immersion in PBS resulting in reduction in the rate at which mass was lost from the cement [20]. It has been reported that formation of HA in brushite cement can occur as early as 72 h after initial immersion in PBS, reaching complete conversion within 19 days of ageing [29]. In our *in vitro* and *in vivo* experiments this early conversion of brushite grafts was not observed. The late conversion of brushite phase to a mixture of OCP and HA observed in this study can be attributed to the *in vitro* media refreshment performed daily and fluid turnover *in vivo* after subcutaneous implantation.

The presence of calcium in serum reduces the solubility of brushite cements [30]. However, we did not observe this reduction in solubility when the grafts were aged in bovine serum. Conversion of brushite cements to HA has been reported previously *in*

vivo [18, 29], and therefore this could be expected after ageing in bovine serum as well. As there was no HA detected at any time point investigated it appeared that serum constituents inhibited apatite formation. Several studies have reported that proteins depending on their types and levels can either inhibit or encourage the formation of HA or its precursor (OCP) in calcium phosphates [9, 31]. It has also been observed that the proteins present in serum can adsorb onto cement surfaces, altering interfacial properties of the crystals [32], favoring *in vitro* resorption. It has already been demonstrated *in vitro* previously that albumin retards the transformation of brushite to HA [28, 33]. The precise role albumin plays in this regard is not known and other proteins present in serum may also play a role in this phenomenon. Since serum contains all of the proteins and ionic constituents that are present *in vivo*, other factors such as enzymes or cellular activity may be responsible for HA formation in brushite cements after implantation. These observations are also supported by the results from our *in vivo* study which demonstrated phase conversion of brushite to OCP & HA after subcutaneous implantation (Fig. 4).

Following subcutaneous implantation, the retrieved monetite grafts had a notably darker appearance compared with the brushite grafts retrieved, suggesting a greater degree of protein adsorption (Fig. 2). However doubt remains as to whether this observation was related to inhibition of HA formation since inhibition was also observed during protein-free PBS incubation (Fig. 3). Further experiments specifically aimed towards determining the reasons for non-conversion of monetite to HA need to be conducted reveal the cause of this effect. A major factor that affects the aqueous chemistry of calcium phosphate cements is the pH [34], and it would be helpful in future

to monitor the pH changes occurring in the incubation media to see how this affects the phase conversion and dissolution.

The results from our study showed that monetite grafts although having lower solubility than brushite cements [8], still resorbed faster *in vivo* (Table 2 and Fig. 7). This was also observed in other recent studies [9, 24]. The mechanism of *in vivo* resorption of monetite cements is similar to that of brushite, with cellular activity accounting for most of the resorption with passive dissolution being less crucial [23]. The possible reason for the monetite grafts showing greater resorption *in vivo* could be the greater total porosity present than brushite. It has been reported that materials with macroporosity can be invaded by resorbing cells and show an increase in the rate and amount of resorption [35]. In light of the greater total porosity and macroporosity present in monetite in comparison to brushite one can envisage that monetite would resorb to a greater extent than brushite. The subcutaneous *in vivo* model used in this study has the inherent limitation of not having osteoclast mediated resorption which would be observed in a bone implantation model. Different resorption behaviour may be expected in a clinically relevant bone defect model and additional work needs to be carried out to evaluate this.

4.2 Disintegration

It was observed that a large proportion of mass lost in PBS and serum for cement grafts prepared with P/L ratio of 1 (Fig. 6c & d) could be attributed to disintegration of the cements due to their highly porous and mechanically weak structure (Table 1) rather than dissolution. This mass loss due to disintegration has also been noted in other *in vitro* [20] and also *in vivo* [29] studies. The fragmentation of high porosity monetite grafts in our

experiments was observed with serum solutions collected every day having murky appearance and particulate matter that collected at the bottom. This was a result of disintegration and release of particulate matter from the cements. XRD analysis revealed that the materials collected were DCPA from the monetite grafts (Fig. S8). This indicates that the particulate matter collected after incubation were likely fragments originating from the ageing sample. The SEM micrograph obtained for the monetite fragments showed crystals mostly in the ~ 2-4 μm size range (Fig. S8), again similar in appearance to that observed for monetite grafts prior to ageing in serum (Fig. 5e). As a consequence of this physical disintegration, the higher porosity brushite grafts lost mass throughout the experiment at a constant rate (Fig. 6c & d). The greater mass loss of the brushite and monetite cements prepared with P/L ratio of 1 when compared with cements prepared with P/L ratio 3 and aged in serum and PBS is thought to be due to higher relative porosity of the P/L ratio 1 grafts. The differences in weight loss observed for the less porous brushite and monetite cements (Table 2) could be attributed to the difference in the solubility constants and not so much dependent upon fragmentation or disintegration of the cement matrix.

4.3 Physical properties

The density of the brushite grafts (Table 1) was higher than what is expected from phase pure brushite (2.27 g/cm^3) [8]. This is due to the presence of small amounts of β-TCP (3.14 g/cm^3) in the brushite cement grafts. The monetite grafts prepared by the two different conversion methods from brushite had lower density (Table 1) than the pure form of monetite (2.92 g/cm^3) [8], indicating some trace amounts of brushite cement

remained unconverted. The increase in the SSA (Table 1) observed after conversion of brushite to monetite was due to the autoclaving process resulting in smaller sized monetite crystals (Fig. 5a & 5c) and an increase in total porosity percentage (Table 1). The brushite cement grafts converted to monetite by dry heating under vacuum demonstrated a greater increase in the SSA (Table 1) and this was observed via SEM imaging (Fig. 5i) which shows decreased size of crystals in comparison with the autoclaved monetite crystals. However, this significant increase in SSA for the dry heat monetite grafts did not enhance *in vivo* resorption or mass loss *in vitro* when compared with the autoclaved monetite grafts.

The relationship between porosity and strength is inversely logarithmic [36, 37]; thus the effect of increase in relative porosity resulted in the loss of compressive strength observed (Table 1). Relative porosity, crystal morphology, degree of conversion, homogeneity of the cement matrix, compaction of the setting cement and critical flaw size are a number of factors which may influence cement strength [38-41]. The highest wet compressive strength value measured for our prepared cement grafts was for the brushite cylinders prepared with P/L ratio of 3 being ~16 MPa (Table 1). The highest compressive strength of ~52 MPa has been reported in literature for hand mixed brushite cements [36]. The reduction in compressive strength observed after ageing was caused by dissolution of the brushite cement that resulted in an increase in the relative porosity *in vitro* and *in vivo* (Fig. S1 and Fig. S2). Mirtchi *et al.* have reported a similar reduction in compressive strength in brushite cements formed from β-TCP and MCPM following ageing in water [42]. A significant reduction in the compressive strength was also noted upon the conversion of brushite grafts to monetite by autoclaving (Table 1). The

detrimental effect on mechanical properties can be attributed to the increase in the relative porosity observed after autoclaving. This increase in porosity and the decrease in mechanical strength is likely one of the reasons for monetite grafts showing greater resorption *in vivo* and mass loss *in vitro*. Interestingly, the brushite grafts converted to monetite by dry heating demonstrated a much higher compressive strength in comparison to their autoclaved counterparts (Table 1) and did not exhibit as great a loss of compressive strength after ageing and implantation. The dry heating process under vacuum not only converts brushite to monetite but also crystals get aggregated as observed by the SEM micrographs (Fig. 5i). This aggregation and interlocking of monetite crystals resulted in the higher compressive strength observed. These dry heat prepared monetite grafts had lower porosity in comparison to their autoclave prepared counterparts and this resulted in comparatively less resorption *in vivo* and mass loss after *in vitro* ageing.

5. Conclusion

This study shows that serum inhibits both the dissolution of brushite and the formation of HA in brushite cement. Serum alters the interfacial properties of the brushite graft surface and this reduces the solubility possibly blocking apatite formation. Further investigation would be required to confirm this. Monetite cements produced by autoclaving and dry heating methods do not demonstrate any phase conversion when aged in PBS or serum. The phenomenon of non-conversion of monetite to apatite in PBS, serum and *in vivo* might be related to how low the pH levels are after monetite dissolution occurs in comparison with brushite. In future research there is a need to monitor pH changes in

order to able to come to a definitive conclusion. While surface area does not play a significant role, disintegration and fragmentation of grafts seems to be the main factors which dictate mass loss in high porosity bioceramics. For cements having lower porosity, solubility plays a more crucial role towards mass loss during *in vitro* ageing and *in vivo* resorption. It appears that it is not only the material composition that dictates cement behavior *in vitro* and *in vivo*, but is a combination of various physical and chemical characteristics. Cement removal from implant site is a complex phenomenon and dependent on a variety of physiologic processes other than simple dissolution. The results obtained from this study lays down the ground work for further investigation to obtain a better understanding of the degradation processes and hence achieving the possibility of graft preparation with higher clinical efficacy.

Acknowledgements

The authors acknowledge financial support from RSBO, Quebec Government MDEIE Catalonia-Quebec grant.

Figure legends:

Fig. 1. Pore size distribution of (a) 3:1 P/L ratio brushite, autoclaved monetite and dry heat monetite grafts, and (b) 1:1 P/L ratio brushite, autoclaved monetite and dry heat monetite grafts.

Fig. 2. Photographs of the retrieved brushite, dry heat monetite and autoclaved monetite grafts after 4 weeks of implantation (a,b,c) and after 12 weeks (d,e,f) [yellow dotted lines denote 6 x 12mm initial dimensions of the grafts]. Radiographs showing brushite (right) and autoclaved monetite (left), (g) upon implantation, (h) after 4 weeks, and (i) after 12 weeks *in vivo*. The monetite grafts were clearly a darker color compared to the brushite grafts indicating greater amount of protein adsorption.

Fig. 3. X-ray diffraction patterns indicating the initial and post ageing in PBS phase composition of brushite, autoclaved and dry heat monetite grafts. Grafts initially consisted of phase pure DCPD (*). The dry heat and autoclaved monetite grafts show the conversion from DCPD to DCPA (†). After ageing in PBS for 60 days the brushite shows conversion from DCPD to OCP (O) and HA (X) and remnants of DCPD. The dry heat and autoclaved monetite grafts do not show any phase change upon ageing in PBS for 60 days.

Fig. 4. X-ray diffraction patterns showing phase composition before and post implantation of:
a. Brushite graft cylinders. The grafts initially consisted of phase pure DCPD (*). After 12 weeks of subcutaneous implantation, the analysis of the grafts revealed the presence of

a mixture of OCP (O), HA (X) and remnants of DCPD. (The surface and core of the grafts retrieved after 12 weeks were analysed).
b. Autoclaved and dry heat monetite grafts. Analysis of both monetite grafts confirmed conversion from DCPD to DCPA (†) before implantation. The autoclaved and dry heat monetite grafts did not show any phase change upon implantation for 12 weeks. (The surface and core of the grafts retrieved after 12 weeks were analysed).

Fig. 5. SEM images obtained from the surface of brushite (a, b, c, d), autoclaved monetite (e, f, g, h) and dry heat monetite (i, j, k, h) grafts before and after immersion in PBS, serum, and subcutaneous implantation in rats on Days 0, 60, and 84 respectively (Scale bars represent 5µm).

Fig. 6. Mass loss of grafts *in vitro* for up to 60 days; (a) 3:1 P/L ratio brushite and monetite grafts in PBS, (b) 3:1 P/L ratio brushite and monetite grafts in serum, (c) 1:1 P/L ratio brushite and monetite grafts in PBS, and (d) 1:1 P/L ratio brushite and monetite grafts in serum.

Fig. 7. Comparison between mass loss of all bioceramic grafts implanted subcutaneously.

Tables:

Table 1. Summary of physicochemical properties of brushite, autoclaved and dry heat converted monetite.

Table 2. Summary of the total percentage of mass loss of brushite and monetite cements after *in vitro* ageing in PBS and bovine serum and after subcutaneous implantation.

Table 3. Summary of changes in calcium-to-phosphorous ratio of brushite and monetite grafts after ageing in PBS, serum, and subcutaneous implantation.

Supplementary figure legends:

Fig. S1. Effect of *in vitro* ageing on relative porosity of, (a) 3:1 P/L ratio grafts in PBS; (b) 3:1 P/L ratio grafts in serum; (c) 1:1 P/L ratio grafts in PBS; and (d) 1:1 P/L ratio grafts in serum. (Grey-brushite, Blue- autoclaved monetite, and Red-dry heat monetite).

Fig. S2. Effect of subcutaneous implantation on relative porosity of, (a) 3:1 P/L ratio grafts, and (b) 1:1 P/L ratio grafts. (Grey-brushite, Blue- autoclaved monetite, and Red-dry heat monetite).

Fig. S3. Effect of *in vitro* ageing on specific surface area (SSA) of, (a) 3:1 P/L ratio grafts in PBS; (b) 3:1 P/L ratio grafts in serum; (c) 1:1 P/L ratio grafts in PBS; and (d) 1:1 P/L ratio grafts in serum. (Grey-brushite, Blue- autoclaved monetite, and Red-dry heat monetite).

Fig. S4. Effect of subcutaneous implantation on specific surface area (SSA) of, (a) 3:1 P/L ratio grafts, and (b) 1:1 P/L ratio grafts. (Grey-brushite, Blue- autoclaved monetite, and Red-dry heat monetite).

Fig. S5. Effect of *in vitro* ageing on density of, (a) 3:1 P/L ratio grafts in PBS; (b) 3:1 P/L ratio grafts in serum; (c) 1:1 P/L ratio grafts in PBS; and (d) 1:1 P/L ratio grafts in serum. (Grey-brushite, Blue- autoclaved monetite, and Red-dry heat monetite).

Fig. S6. Effect of subcutaneous implantation on density of, (a) 3:1 P/L ratio grafts, and (b) 1:1 P/L ratio graft. (Grey-brushite, Blue- autoclaved monetite, and Red-dry heat monetite).

Fig. S7. X-ray diffraction pattern indicating the phase composition of brushite graft after 12 weeks of ageing in PBS. The characteristic peak of 4.75º 2θ (O) indicates OCP.

Fig. S8. (A) SEM image of the disintegration products/fragments collected from the monetite grafts incubated in serum (Scale bars represent 20 µm). (B) X-ray diffraction pattern indicating the phase composition of disintegration products/fragments collected from the monetite grafts incubated in serum († represents monetite peaks).

References

[1] Lemaitre J, Mirtchi AA, Mortier A. Calcium phosphate cements for medical use: state of the art and perspectives of development. Silicates Industriels 1987;10:141-6.
[2] Bohner M. Calcium orthophosphates in medicine: from ceramics to calcium phosphate cements. Injury 2000;31:37-47.
[3] Mirtchi AA, Lemaitre J, Munting E. Calcium-phosphate cements - effect of flourides on the setting and hardening of beta-tricalcium phosphate dicalcium phosphate calcite cements. Biomaterials 1991;12:505-10.
[4] Mirtchi AA, Lemaitre J, Munting E. Calcium-phosphate-cements - Action of setting regulators on the properties of the beta-tricalcium phosphate monocalcium phosphate cements. Biomaterials 1989;10:634-8.
[5] Mirtchi AA, Lemaitre J, Munting E. Calcium-phosphate-cements- Study of the beta-tricalcium phosphate dicalcium phosphate calcite cements Biomaterials 1990;11:83-8.
[6] Bohner M, Merkle HP, Lemai, tre J. In vitro aging of a calcium phosphate cement. Journal of Materials Science: Materials in Medicine 2000;11:155-62.
[7] Alshaaer M, Cuypers H, Rahier H, Wastiels J. Production of monetite-based Inorganic Phosphate Cement (M-IPC) using hydrothermal post curing (HTPC). Cement and Concrete Research 2011;41:30-7.
[8] Tamimi F, Sheikh Z, Barralet J. Dicalcium phosphate cements: brushite and monetite. Acta Biomater 2012;8:474-87.
[9] Tamimi F, Le Nihouannen D, Eimar H, Sheikh Z, Komarova S, Barralet J. The effect of autoclaving on the physical and biological properties of dicalcium phosphate dihydrate bioceramics: brushite vs. monetite. Acta Biomater 2012;8:3161-9.
[10] Penel G, Leroy G, Leroy N, Behin P, Langlois JM, Libersa JC, et al. Raman spectrometry applied to calcified tissue and calcium-phosphorus biomaterials. Bull Group Int Rech Sci Stomatol Odontol 2000;42:55-63.
[11] Constantz BR, Barr BM, Ison IC, Fulmer MT, Baker J, McKinney L, et al. Histological, chemical, and crystallographic analysis of four calcium phosphate cements in different rabbit osseous sites. J Biomed Mater Res 1998;43:451-61.
[12] Tamimi F, Torres J, Al-Abedalla K, Lopez-Cabarcos E, Alkhraisat MH, Bassett DC, et al. Osseointegration of dental implants in 3D-printed synthetic onlay grafts customized according to bone metabolic activity in recipient site. Biomaterials 2014.
[13] Tamimi F, Torres J, Bassett D, Barralet J, Cabarcos EL. Resorption of monetite granules in alveolar bone defects in human patients. Biomaterials 2010;31:2762-9.
[14] Tamimi F, Torres J, Gbureck U, Lopez-Cabarcos E, Bassett DC, Alkhraisat MH, et al. Craniofacial vertical bone augmentation: a comparison between 3D printed monolithic monetite blocks and autologous onlay grafts in the rabbit. Biomaterials 2009;30:6318-26.
[15] Tamimi F, Torres J, Kathan C, Baca R, Clemente C, Blanco L, et al. Bone regeneration in rabbit calvaria with novel monetite granules. Journal of Biomedical Materials Research Part A 2008;87A:980-5.
[16] Ohura K, Bohner M, Hardouin P, Lemaitre J, Pasquier G, Flautre B. Resorption of, and bone formation from, new beta-tricalcium phosphate-monocalcium phosphate cements: An in vivo study. Journal of Biomedical Materials Research 1996;30:193-200.
[17] Frayssinet P, Gineste L, Conte P, Fages J, Rouquet N. Short-term implantation effects of a DCPD-based calcium phosphate cement. Biomaterials 1998;19:971-7.

[18] Flautre B, Delecourt C, Blary MC, Van Landuyt P, Lemaitre J, Hardouin P. Volume effect on biological properties of a calcium phosphate hydraulic cement: Experimental study in sheep. Bone 1999;25:35S-9S.
[19] Grover LM, Gbureck U, Wright AJ, Tremayne M, Barralet JE. Biologically mediated resorption of brushite cement in vitro. Biomaterials 2006;27:2178-85.
[20] Grover LM, Knowles JC, Fleming GJP, Barralet JE. In vitro ageing of brushite calcium phosphate cement. Biomaterials 2003;24:4133-41.
[21] Theiss F, Apelt D, Brand BA, Kutter A, Zlinszky K, Bohner M, et al. Biocompatibility and resorption of a brushite calcium phosphate cement. Biomaterials 2005;26:4383-94.
[22] Kuemmerle JM, Oberle A, Oechslin C, Bohner M, Frei C, Boecken I, et al. Assessment of the suitability of a new brushite calcium phosphate cement for cranioplasty - an experimental study in sheep. Journal of Cranio-Maxillofacial Surgery 2005;33:37-44.
[23] Grossardt C, Ewald A, Grover LM, Barralet JE, Gbureck U. Passive and Active In Vitro Resorption of Calcium and Magnesium Phosphate Cements by Osteoclastic Cells. Tissue Engineering Part A 2010;16:3687-95.
[24] Gbureck U, Hozel T, Klammert U, Wurzler K, Muller FA, Barralet JE. Resorbable dicalcium phosphate bone substitutes prepared by 3D powder printing. Advanced Functional Materials 2007;17:3940-5.
[25] Alkhraisat MH, Marino FT, Retama JR, Jerez LB, Lopez-Cabarcos E. Beta-tricalcium phosphate release from brushite cement surface. Journal of Biomedical Materials Research Part A 2008;84A:710-7.
[26] Lu J DM, Dejou J, Koubi G, Hardouin P, Lemaitre J, Proust JP. The biodegradation mechanism of calcium phosphate biomaterials in bone. J Biomed Mater Res 2002;63:408-12.
[27] Kumar M DH, Riley C. . Electrodeposition of brushite coatings and their transformation to hydroxyapatite in aqueous solutions. J biomed Mater Res 1999;45:302-10.
[28] Xie J RC, Chittur K. Effect of albumin on brushite transformation to hydroxyapatite. J biomed Mater Res 2001;57:357-65.
[29] Constantz BR, Barr BM, Ison IC, Fulmer MT, Baker J, McKinney LA, et al. Histological, chemical, and crystallographic analysis of four calcium phosphate cements in different rabbit osseous sites. Journal of Biomedical Materials Research 1998;43:451-61.
[30] Bohner M, vanLanduyt P, Merkle HP, Lemaitre J. Composition effects on the pH of a hydraulic calcium phosphate cement. Journal of Materials Science-Materials in Medicine 1997;8:675-81.
[31] Maria SM, Prukner C, Sheikh Z, Mueller F, Barralet JE, Komarova SV. Reproducible quantification of osteoclastic activity: Characterization of a biomimetic calcium phosphate assay. J Biomed Mater Res B Appl Biomater 2013.
[32] Giocondi JL, El-Dasher BS, Nancollas GH, Orme CA. Molecular mechanisms of crystallization impacting calcium phosphate cements. Philosophical Transactions of the Royal Society a-Mathematical Physical and Engineering Sciences 2010;368:1937-61.
[33] Steinberg D KA, Kohavi D, Sela MN. Adsorption of human salivary proteins to titanium powder. Biomaterials 1995;16:1339-43.
[34] Chow LC. Development of self-setting calcium phosphate cements. The Centennial Memorial Issue of The Ceramic Society of Japan 1991;99:954-64.
[35] Bohner M, Baumgart F. Theoretical model to determine the effects of geometrical factors on the resorption of calcium phosphate bone substitutes. Biomaterials 2004;25:3569-82.

[36] Hofmann MP, Mohammed AR, Perrie Y, Gbureck U, Barralet JE. High-strength resorbable brushite bone cement with controlled drug-releasing capabilities. Acta Biomaterialia 2009;5:43-9.
[37] Van Landuyt P, Lowe C, Lemaitre J. Optimization of setting time and mechanical strength of beta-TCP/MCPM cements. Bioceramics, Vol 10 1997:477-80.
[38] Ishikawa K TS, Chow LC, Suzuki K. Reaction of calcium phosphates with different amounts of tetracalcium phosphate and dicalcium phosphate anhydrous. . J Biomed Mater Res B Appl Biomater 1999;46:504-10.
[39] Ishikawa K AK. Estimation of ideal mechanical strength and critical porosity of calcium phosphate cement. . J biomed Mater Res 1995;29:1537-43.
[40] Tamimi F, Sheikh Z, Barralet J. Dicalcium phosphate cements: Brushite and monetite. Acta Biomaterialia 2012;8:474-87.
[41] Barralet JE, Grover LM, Gbureck U. Ionic modification of calcium phosphate cement viscosity. Part II: hypodermic injection and strength improvement of brushite cement. Biomaterials 2004;25:2197-203.
[42] Mirtchi AA, Lemaitre J, Terao N. Calcium phosphate cements: study of the beta-tricalcium phosphate-monocalcium phosphate system. . Biomaterials 1989;10:475-80.

Graft type and P/L ratio	Porosity (%)	S.S.A (m^2/g)	Density (g/cm^3)	Compressive strength (MPa)
3:1 Brushite	36 ± 1.75	0.62 ± 0.18	2.42 ± 0.05	16.6 ± 0.88
3:1 AC monetite	53 ± 1.75	1.66 ± 0.08	2.87 ± 0.02	8.1 ± 1.14
3:1 DH monetite	45 ± 2.63	20.05 ± 1.00	2.85 ± 0.04	15.0 ± 1.40
1:1 Brushite	65 ± 1.75	0.89 ± 0.11	2.45 ± 0.04	8.4 ± 0.96
1:1 AC monetite	60 ± 2.63	1.12 ± 0.11	2.89 ± 0.04	2.4 ± 0.70
1:1 DH monetite	60 ± 1.75	19.36 ± 1.55	2.83 ± 0.08	5.3 ± 0.53

Data presented as average values with confidence intervals (95%)
AC- Autoclaved
DH- Dry heat
S.S.A - Specific surface area

Biomaterial (P/L ratio)	PBS 60 days (mass loss %)	Serum 60 days (mass loss %)	Subcutaneous 84 days (mass loss %)
3:1 Brushite	13 ±1.13	16 ±1.13	17 ± 1.6
3:1 DH monetite	10 ±1.70	12.5 ±1.13	25 ± 2.0
3:1 AC monetite	4.5 ± 0.57	7 ± 0.57	30 ± 1.6
1:1 Brushite	26 ±2.26	42.5 ± 2.26	29 ± 2.4
1:1 DH monetite	29 ±1.70	37 ± 3.26	39 ± 1.6
1:1 AC monetite	33 ±1.70	47 ± 1.70	48 ± 3.6

Data presented as average values with confidence intervals (95%)
AC- Autoclaved
DH- Dry heat
S.S.A - Specific surface area

Biomaterial	Before experiments	PBS (60 days)	Serum (60 days)	Subcutaneous (84 days)
3:1 Brushite	1.10 ± 0.07	1.42 ± 0.09*	1.10 ± 0.12	1.59 ± 0.15*
1:1 Brushite	1.04 ± 0.10	1.38 ± 0.08*	1.15 ± 0.08	1.51 ± 0.09*
3:1AC monetite	1.17 ± 0.05	1.13 ± 0.07	1.14 ± 0.01	1.23 ± 0.07
1:1AC monetite	1.15 ± 0.09	1.18 ± 0.09	1.12 ± 0.12	1.31 ± 0.16
3:1 DH monetite	1.13 ± 0.06	1.11 ± 0.14	1.11 ± 0.14	1.23 ± 0.01
1:1 DH monetite	1.06 ± 0.11	1.15 ± 0.11	1.14 ± 0.06	1.21 ± 0.09

Data presented as average values with confidence intervals (95%)
AC- Autoclaved
DH- Dry heat
S.S.A - Specific surface area
(*) signifies the statistical significance of increase in Ca/P ratio from start of experiments ($P < 0.05$)

Figure 1 jpeg

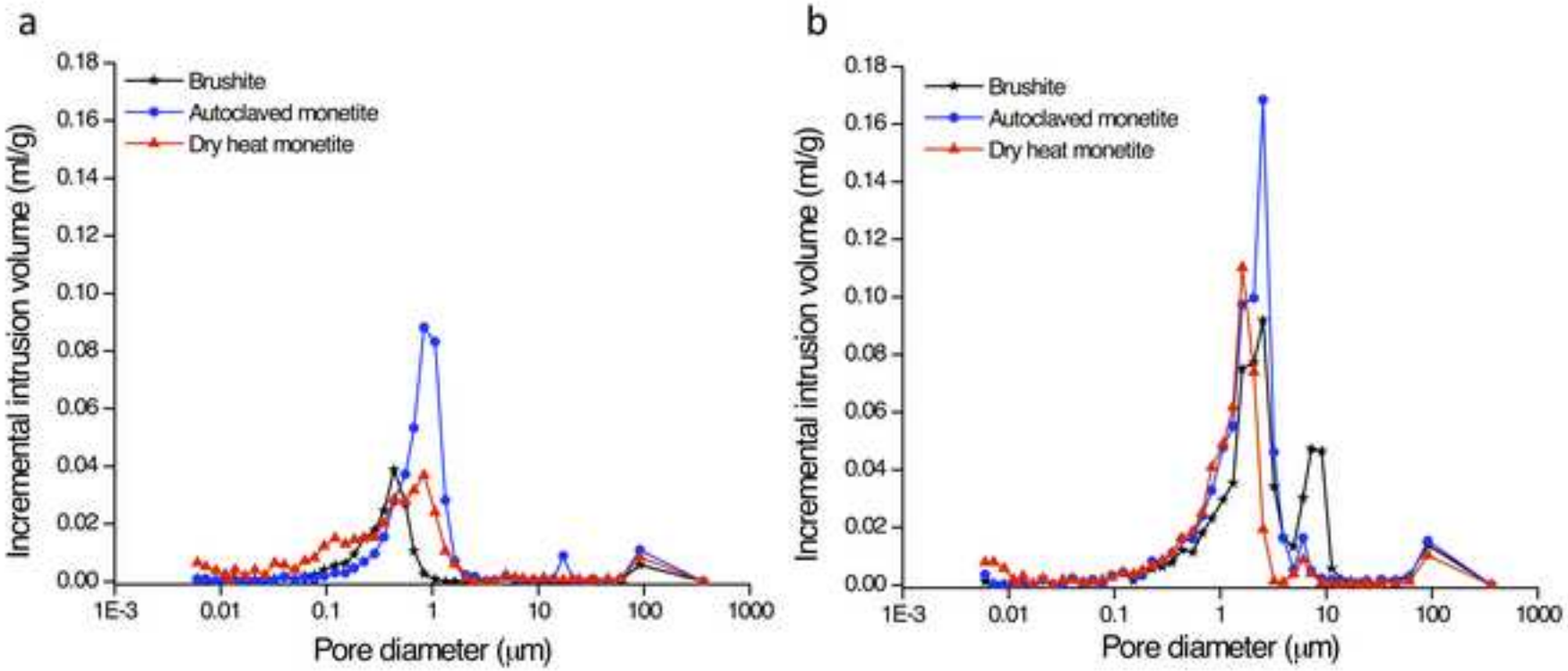

Figure 2 jpeg

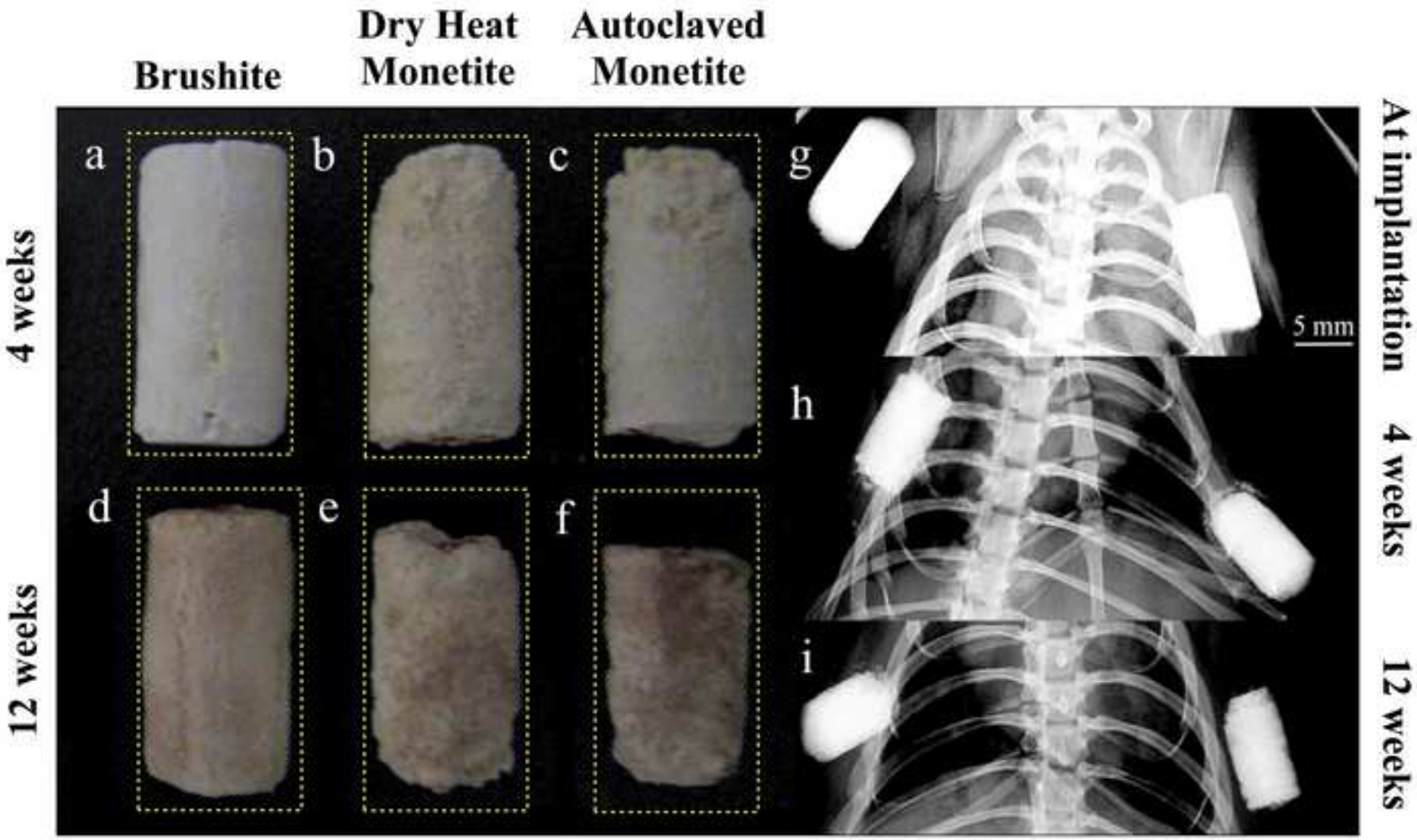

Figure 3 jpeg

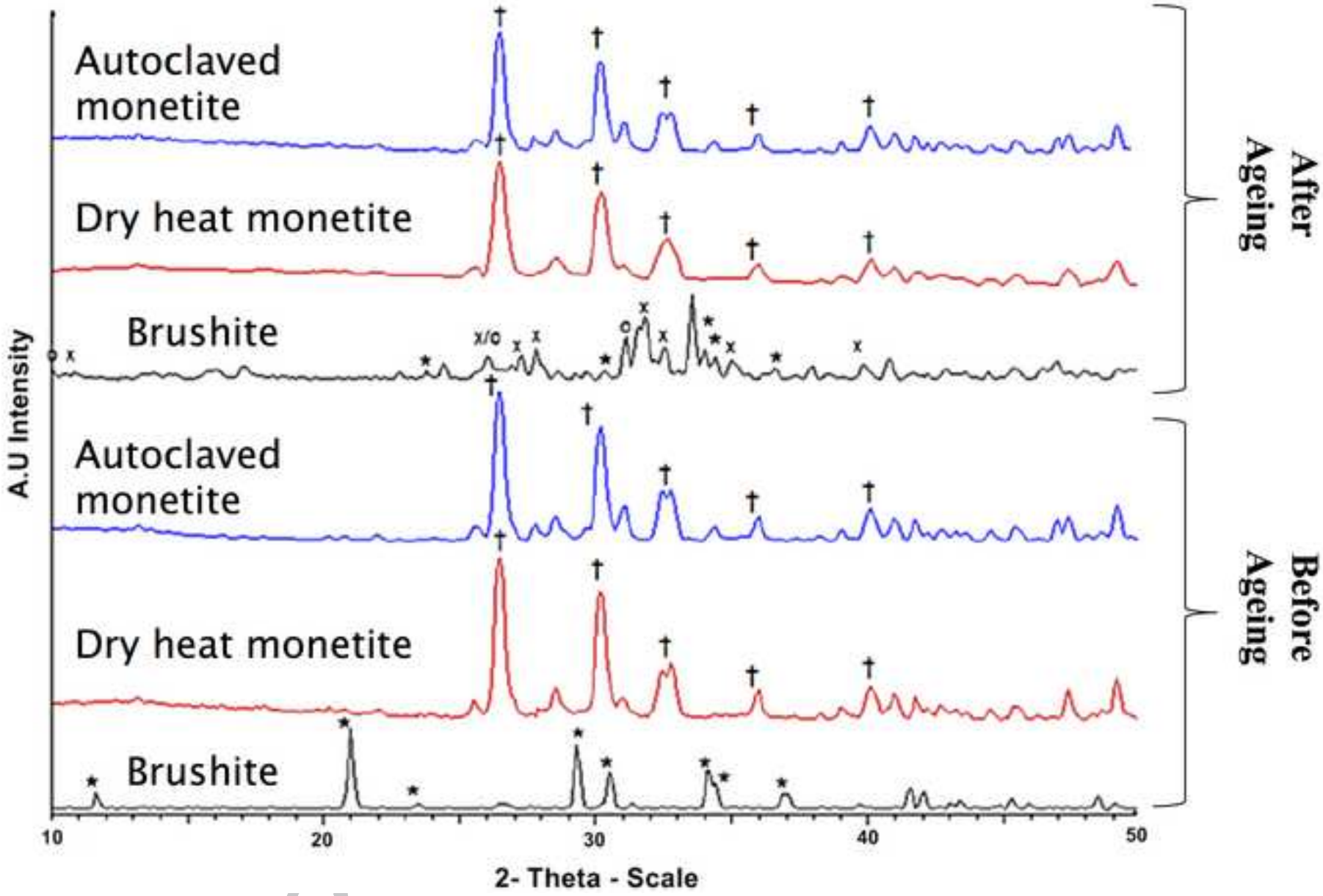

Figure 4 jpeg

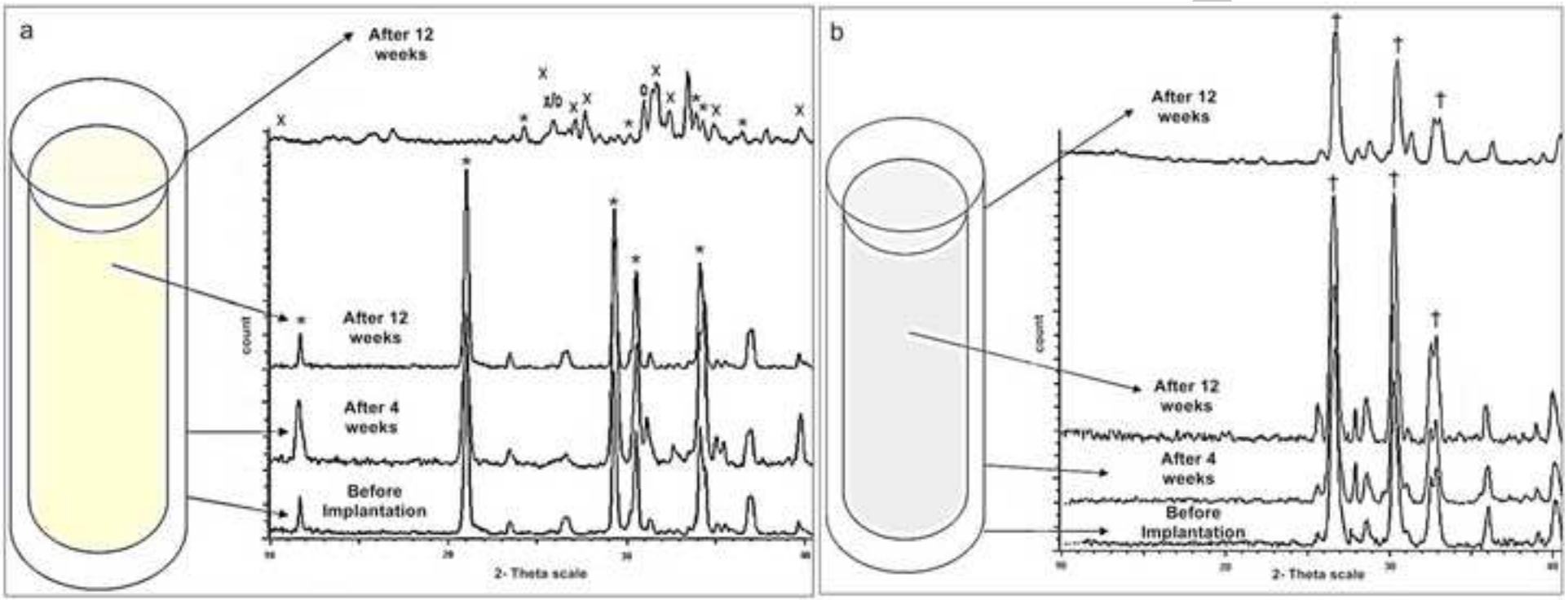

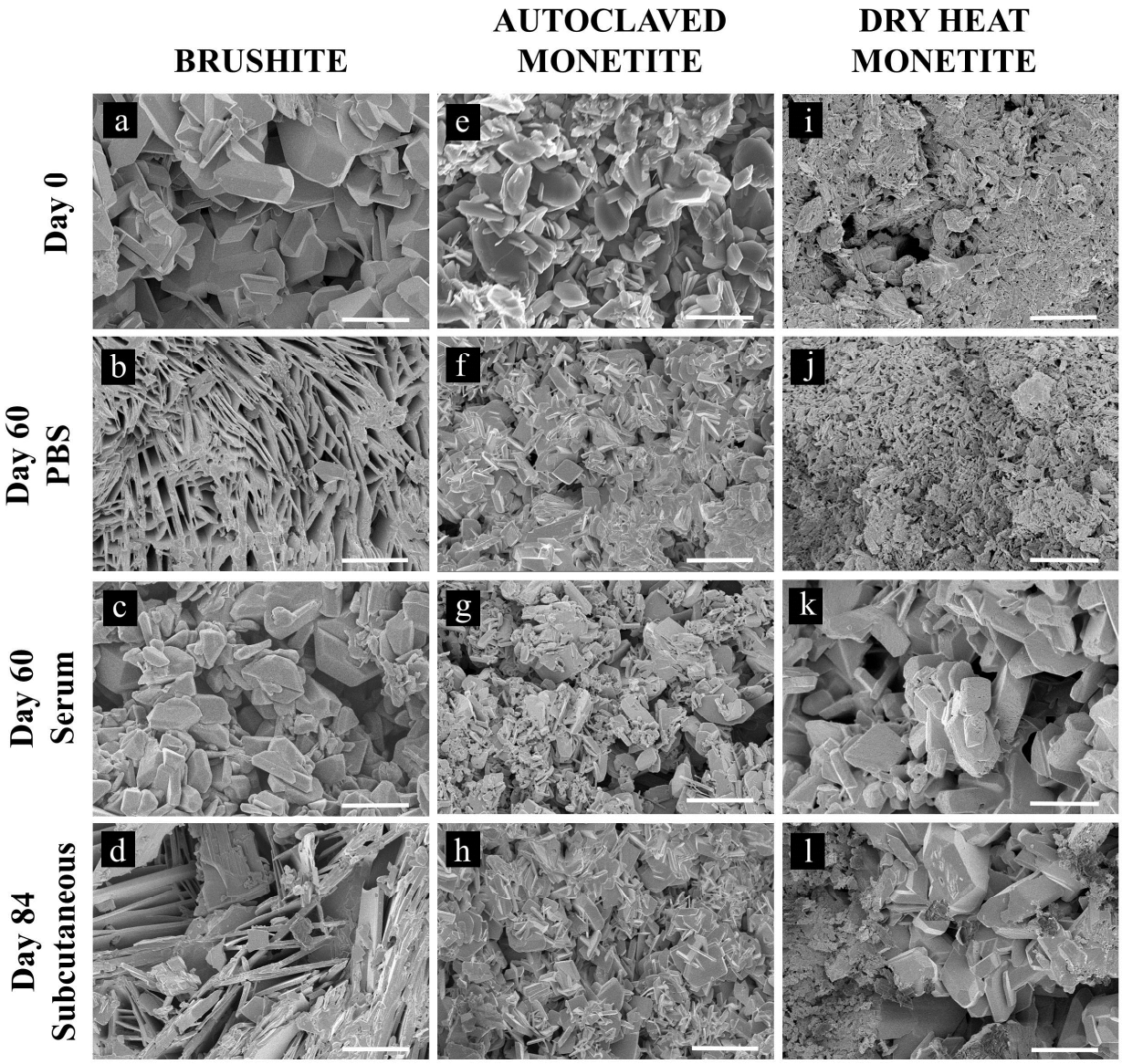
BRUSHITE
AUTOCLAVED MONETITE
DRY HEAT MONETITE
Day 0
Day 60 PBS
Day 60 Serum
Day 84 Subcutaneous
a
b
c
d
e
f
g
h
i
j
k
l

Figure 6 jpeg

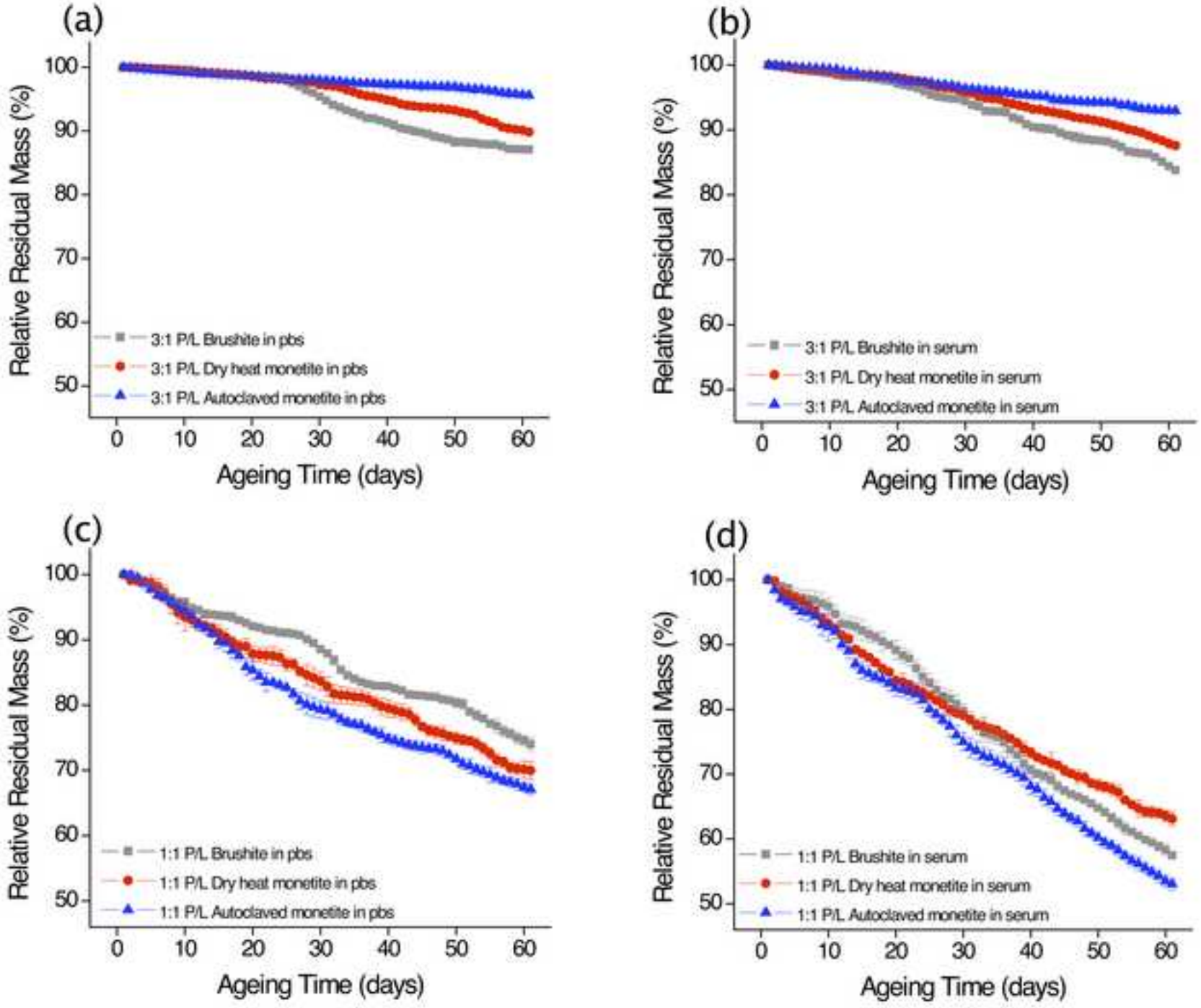

Figure 7 jpeg